2

Real-Time Detection of Infrared Profile Patterns and Features Extraction

Rubén Usamentiaga, Daniel F. García and Julio Molleda
University of Oviedo
Spain

1. Introduction

The pressing demand to improve quality of manufactured products requires the use of the latest technologies in order to enhance the control systems that adjust manufacturing parameters. Computer vision inspection and control are already standard technologies which are frequently used to improve the quality of manufactured products. Recently, due to the availability of fast and affordable infrared acquisition devices, computer vision beyond the spectrum is also becoming an essential technology for quality control and improvement. For example, during steel strips manufacturing, uneven temperature across the width of the strips during rolling generates defects, due to differences in the contraction of the longitudinal fibers that make up a strip. Detecting the infrared profile pattern of the strip which is being manufactured makes it possible to use this information to modify the manufacturing parameters to compensate for the temperature differences in the strip (Gonzalez et al., 2002).

This work proposes a robust method to detect infrared profile patterns in real-time. The proposed method is based on the acquisition and processing of infrared profiles using an infrared line scanner. The detection of infrared patterns, and the change of pattern which occur during manufacturing, need to be carried out online with the production process in order to use this information to enhance the control systems during manufacturing. The method proposed to detect these patterns in real-time is based on the segmentation of the stream of infrared profiles acquired from the infrared line scanner. The segmentation aims to find regions of homogeneous temperature, that is, regions formed by a set of adjacent profiles which have a similar temperature pattern. The proposed method to segment infrared images into regions of common temperature patterns is by means of boundary detection, which, in this case, is accomplished through edge detection. The first step of the segmentation is the calculation of the gradient, which is obtained as the result of the convolution of the image with a gradient operator. Two different gradient operators, Gaussian and difference, are evaluated to test which one is best suited to solve the current problem. The next step is the projection of the gradient, which simplifies the thresholding that must be carried out to eliminate noise from the gradient. Once the projection of the gradient is available, it is thresholded. The objective of the thresholding is to differentiate noise from real edges. An edge is found when there is data in the projection over the

Source: Pattern Recognition Techniques, Technology and Applications, Book edited by: Peng-Yeng Yin,
ISBN 978-953-7619-24-4, pp. 626, November 2008, I-Tech, Vienna, Austria

threshold. All these processes are designed to require low computational power, which makes a real-time implementation possible. The information about the current infrared profile pattern and about the changes in the infrared pattern obtained in real-time can be used to improve the quality of the product during manufacturing.

In addition to real-time detection of infrared profile patterns, methods to extract distinguishing features from infrared patterns are explored in this work. These features aim to characterize infrared patterns to be recognized by measurements whose values are very similar for patterns in the same category, and very different from patterns in different categories. Polynomial fit using orthogonal polynomials is studied as a method capable of providing a compact and meaningful description of infrared profile patterns.

2. Infrared images

Temperature in infrared images is computed from the measured radiation, according to Planck's law. The conversion is affected by the emissivity of the object radiating energy, which is a parameter of the device used to acquire infrared images. Among infrared acquisition devices, infrared line scanners are the most commonly used to measure the temperature of very long moving objects, such as steel strips. Image acquisition using these devices is carried out by capturing infrared profiles from objects which move forward along a track. The repetitive line-scanning (≈100Hz) and the movement of the object make the acquisition of a rectangular image possible. Fig. 1 shows a diagram of the operation of an infrared line scanner.

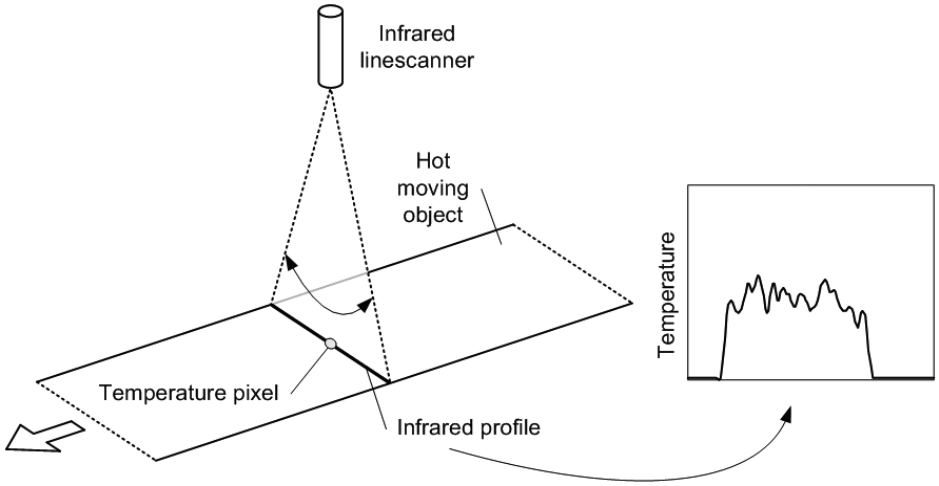

Fig. 1. Operation of an infrared line scanner

The resulting infrared image consists of a sequence of infrared profiles, each of which is made up of a set of pixels which represent temperature. Fig. 2 shows an example of infrared image acquired from a hot steel strip. Infrared images acquired from steel strips using infrared line scanners have an approximated resolution of 130 rows and 10,000 columns, where each pixel of the image represents a temperature value in the range [100, 200ºC].

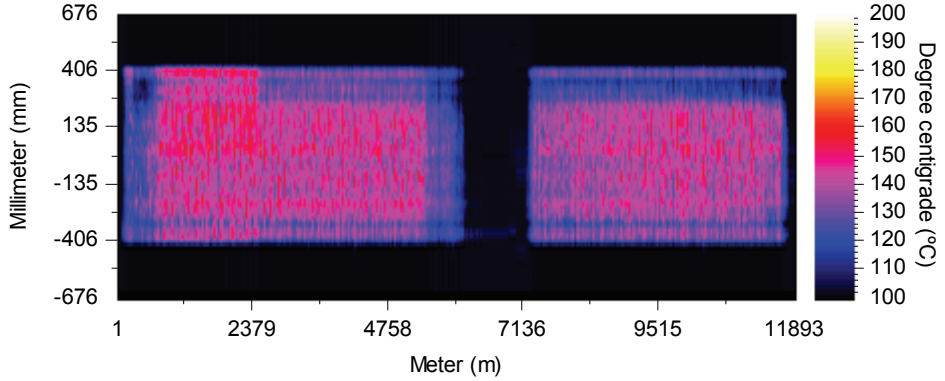

Fig. 2. Example of infrared image acquired from a steel strip

2.1 Infrared profile patterns

One of the objectives of this work is the detection of infrared profile patterns. This means detection regions of homogeneous temperature, that is, regions formed by a set of adjacent profiles which have a similar temperature pattern.

Different regions in the infrared image appear as a consequence of the changes of the manufacturing conditions over time. The following is an example of how different regions can appear in an image acquired from a steel strip. For an instant during a strip manufacturing (Fig. 3, moment A) the speed is reduced, which produces a decrement in the temperature of the strip. Before the speed reduction, the profiles acquired show a high infrared profile pattern (Fig. 3, pattern 1), and after the speed reduction they show a lower one (Fig. 3, pattern 2). Later (Fig. 3, moment B), the speed strip is recovered and the pattern is again high (Fig. 3, pattern 3). After this, a typical change in the manufacturing conditions is produced (Fig. 3, moment C), which consists of the application of excessive pressure on one part of the strip. The excess of pressure generates heat and the infrared pattern rises where high pressure is applied to the strip (Fig. 3, pattern 4). When the excess of pressure disappears (Fig. 3, moment D) a flat infrared pattern appears again (Fig. 3, pattern 5). Finally, a new decrement of the speed (Fig. 3, moment E) produces a new infrared pattern (Fig. 3, pattern 6).

In the case of steel strips, information about the current temperature pattern can be used during the manufacturing process to activate the cooling nozzles where the temperature is higher. However, to do this, infrared profile patterns must be detected in real-time with the manufacturing process, making the real-time adjustment of the cooling feedback possible.

3. Detection of infrared profile patterns

The method proposed to detect these infrared profile patterns in real-time is based on the segmentation of the stream of infrared profiles acquired from the infrared line scanner. The proposed method to segment infrared images into regions of common temperature patterns is by means of boundary detection, which, in this case, is accomplished through edge detection.

Segmentation techniques based on edge detection rely on edges found in an image by edge detection operators. These edges mark image discontinuities regarding some image attribute. Usually, the attribute is the luminance level; in this case, the temperature level will be used.

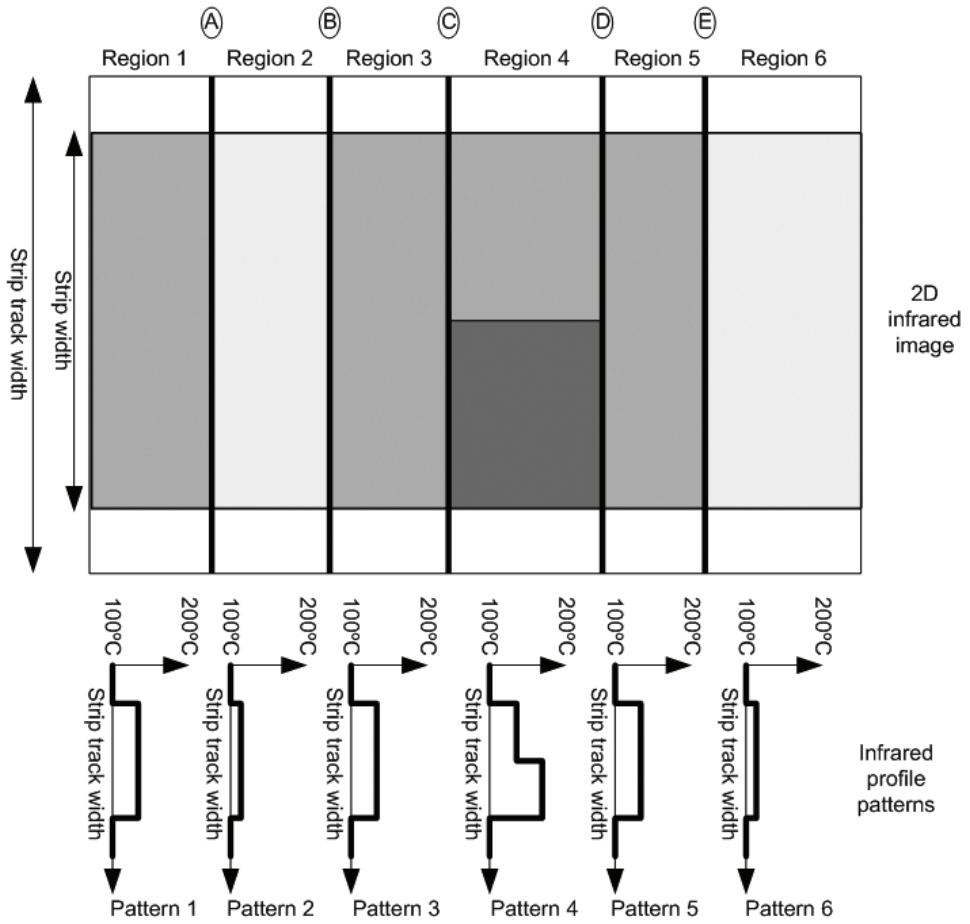

Fig. 3. Infrared profile patterns

The general edge-based segmentation process consists of several steps. It starts by applying a convolution kernel (or gradient operator) over an image (Pratt, 2001). The result obtained from the convolution is the gradient of the image, which is obviously dependent on the gradient operator used. The next step involves the analysis of the gradient in order to eliminate the noise while keeping the real edges. Usually, this process is carried out by using thresholding techniques or morphological operators. The last step consists of linking the edges in order to determine the boundary of the regions, and in this way, to accomplish the segmentation of the image into regions.

The steps for the proposed edge-based segmentation method for the infrared images considered in this work are described below.

3.1 Calculation of the gradient

The gradient of an image is obtained as the result of the convolution of the image with a gradient operator, also called convolution kernel (Canny, 1986).

When choosing a gradient operator, three important issues must be carefully selected: the direction, the size, and the shape. The fact that the edges will only be searched in the direction of the object movement makes the selection of direction and size easier. The direction of the operator will be the same as the object movement, that is, longitudinal. Furthermore, the size, normally defined as A rows x B columns, can be simplified as 1xB, since only the modification of the number of columns of the operator (B) will make significant changes to the resulting gradient. To simplify the next operations, N, defined as (B-1)/2, will be used when referring to the operator length.
In order to decide which operator shape best fits the images considered, two operators were analyzed: the difference operator and the FDoG (first derivative of Gaussian). The difference operator consists of a convolution kernel where the first N coefficients are -1, the next is 0, and the last N are 1. Summarizing, this operator calculates the difference between the next and the previous window (both of size N) of the current pixel. On the other hand, the FDoG operator consists of the derivative of a Gaussian function. The representation of both operators can be seen in Fig. 4.

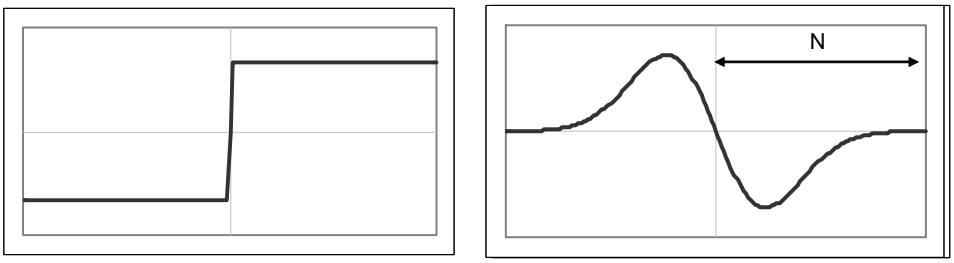

(a) (b)

Fig. 4. Gradient operators. (a) difference, (b) FDoG

To apply the FDoG operator, a convolution operation must be carried out. This operation can be calculated using (1), where LS[i, j] is the pixel j of the infrared profile i, and FDoG[i] is the i^{th} coefficient of the FDoG operator.

$$FDoG\_Grad[i,j] = \sum_{k=i-N}^{k=i+N} LS[k,j]\,FDoG[k-(i-N)] \tag{1}$$

To apply the difference operator (Dif), the same convolution operation with different coefficients can be used. However, since the application of the difference operator in one pixel corresponds to the calculation of the difference between two averages, it can also be applied in Eq. (2).
Eq. (2) can also be seen as (3), the difference between the next and previous window (size N), where ALS[f, t, j] is the average pixel j from the profile f to t.

$$Dif\_Grad[i,j] = \frac{\sum_{k=i+1}^{k=i+N} LS[k,j]}{N} - \frac{\sum_{k=i-N}^{k=i-1} LS[k,j]}{N} \tag{2}$$

$$Dif\_Grad[i,j] = ALS[i+1, i+N, j] - ALS[i-N, i-1, j] \tag{3}$$

The average of a signal from point a to point b can be calculated using Eq. (4), which can be transformed into a recursive equation as seen in Eq. (5).

$$\overline{x_{a,b}} = \frac{\sum_{i=a}^{b} x_i}{b-a+1} \tag{4}$$

$$\overline{x_{a,b}} = \frac{\sum_{i=a-1}^{b-1} x_i + x_b - x_{a-1}}{b-a+1} = \overline{x_{a-1,b-1}} + \frac{x_b - x_{a-1}}{b-a+1} \tag{5}$$

Using the recursive definition of the average given in Eq. (5), Eq. (6) can be proposed for the calculation of ALS, which makes it possible to calculate the operator recursively, therefore requiring a lower number of operations.

$$ALS[a,b,j] = ALS[a-1,b-1,j] + \frac{LS[b,j] - LS[a-1,j]}{b-a+1} \tag{6}$$

The segmentation method must be applied in real-time. This means that the time necessary to calculate the gradient in a profile will be a part of the total time necessary to process a new acquired profile (maximum of 10ms using an infrared line-scanner of 100Hz). Applying a convolution operation with an operator of window size N, and a profile of length L requires the operations included in Table 1. The recursive version is seen to need far fewer mathematical operations than the convolution. For example, the calculations of the gradient using an operator of window size 100 over a profile of 100 points, would need 40,000 mathematical operations using the convolution, but only 700 using the recursive approach. This difference makes the recursive approach 57 times faster than the convolution, which, depending on the computation speed, could represent the difference between being able to calculate the gradient before the deadline or not.

	Convolution	Recursive
Multiplications:	2*N*L	0
Additions:	2*N*L	2*L
Subtraction:	0	3*L
Divisions:	0	2*L
Total:	4*N*L	7*L

Table 1. Number of operations required to calculate the gradient

Fig. 5 shows the gradient produced by the difference and FDoG operators (both using N=100) when applied to the infrared image shown in Fig. 2.

Taking the previous considerations into account, the most suitable operator in this case is the difference, for three reasons:

- The multiple response effect in the produced gradient is not avoided by any of the operators (Canny, 1986).
- The gradient produced by the difference operator maximizes the SNR (signal to noise ratio) (Canny, 1986).

- Since the difference operator can be applied recursively, its implementation is much faster than the convolution operation. This constitutes a significant advantage when designing a segmentation method to work in real time.

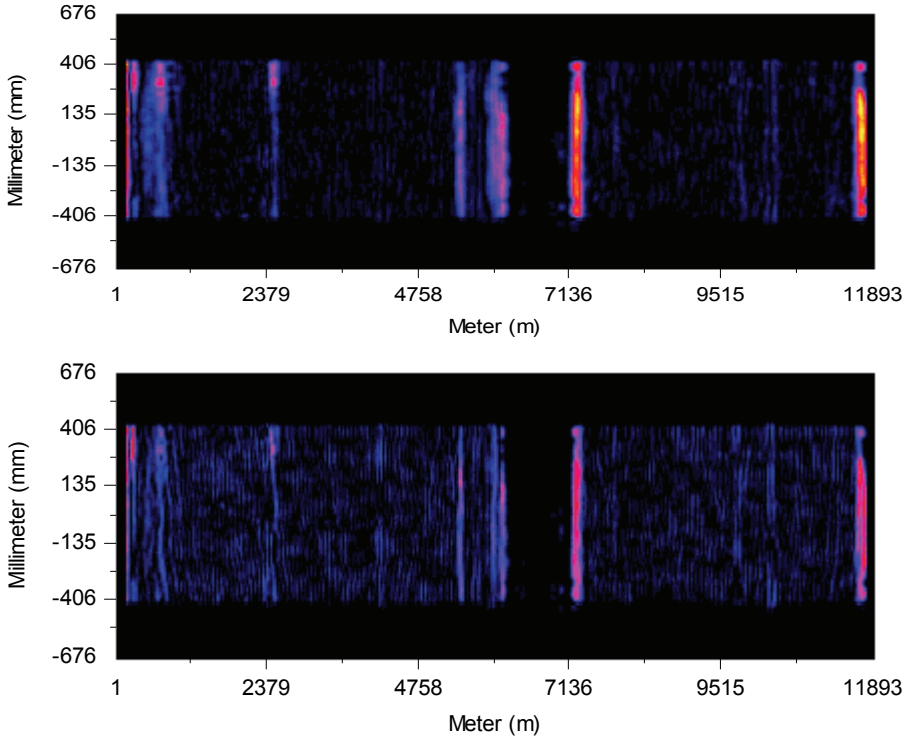

Fig. 5. Gradient produced by the difference (a) and FDoG (b) operators

3.2 Projection of the gradient

The next step is the projection of the gradient, which simplifies the thresholding that must be carried out to eliminate noise from the gradient. This projection is carried out using Eq. (7), where LSL is the profile length (number of pixels in the profile), and P is a parameter of the projection.

$$GradProj[i] = \frac{1}{LSL}\sum_{j=1}^{LSL}\left(Grad[i,j]\right)^{P} \tag{7}$$

Fig. 6 shows the projection (using P=2) of the gradients obtained using the difference and FDoG gradient operators, which can be seen in Fig. 5. This figure shows that the difference operator identifies the edges of the image more clearly and with more responses per edge, which corroborates the conclusions drawn in Canny's work (Canny, 1986) on the proper gradient operator under his constraints of SNR (signal to noise ratio) and simple response.

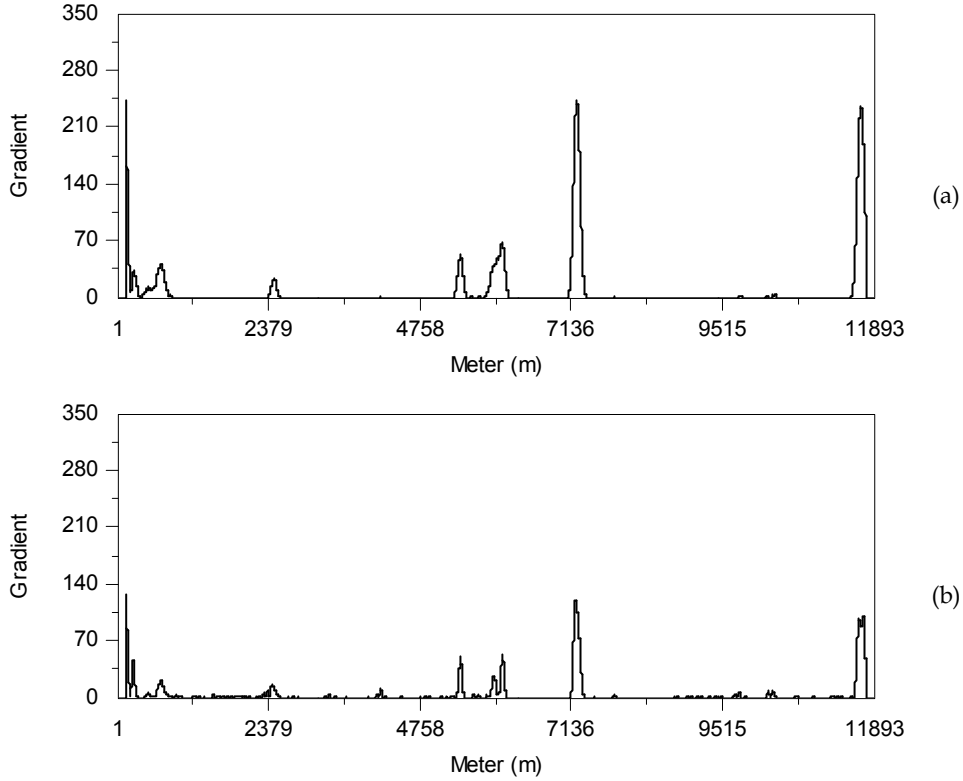

Fig. 6. Projection of the gradient. (a) using difference operator, (b) using FDoG operator

3.3 Thresholding of the projection

Once the projection of the gradient is available, it is thresholded. The objective of the thresholding is to differentiate noise from real edges. An edge is found when there is data in the projection over the threshold value T. When adjacent edges are found (adjacent values of the projection over the threshold), only the edge with the higher value in the projection of all of the adjacent positions will be considered. This can be interpreted as a morphological operator.

Fig. 7a shows an example of the thresholding (T=25) carried out over the projection (P=2) of the gradient produced by the difference operator (N=100, shown in Fig. 6a) over the image in Fig. 2. As can be seen, the noise is below the threshold value and edges are obtained from the peaks above it (Fig. 7b). Only the highest value of each peak will be considered to establish the longitudinal position of its corresponding edge. The segmented image consists of the set of regions bounded by the found edges (Fig. 7c).

3.4 Summary of the segmentation method

The proposed segmentation method for infrared images is based on edge detection. Edges are detected by means of the thresholding of the projection of the gradient calculated with

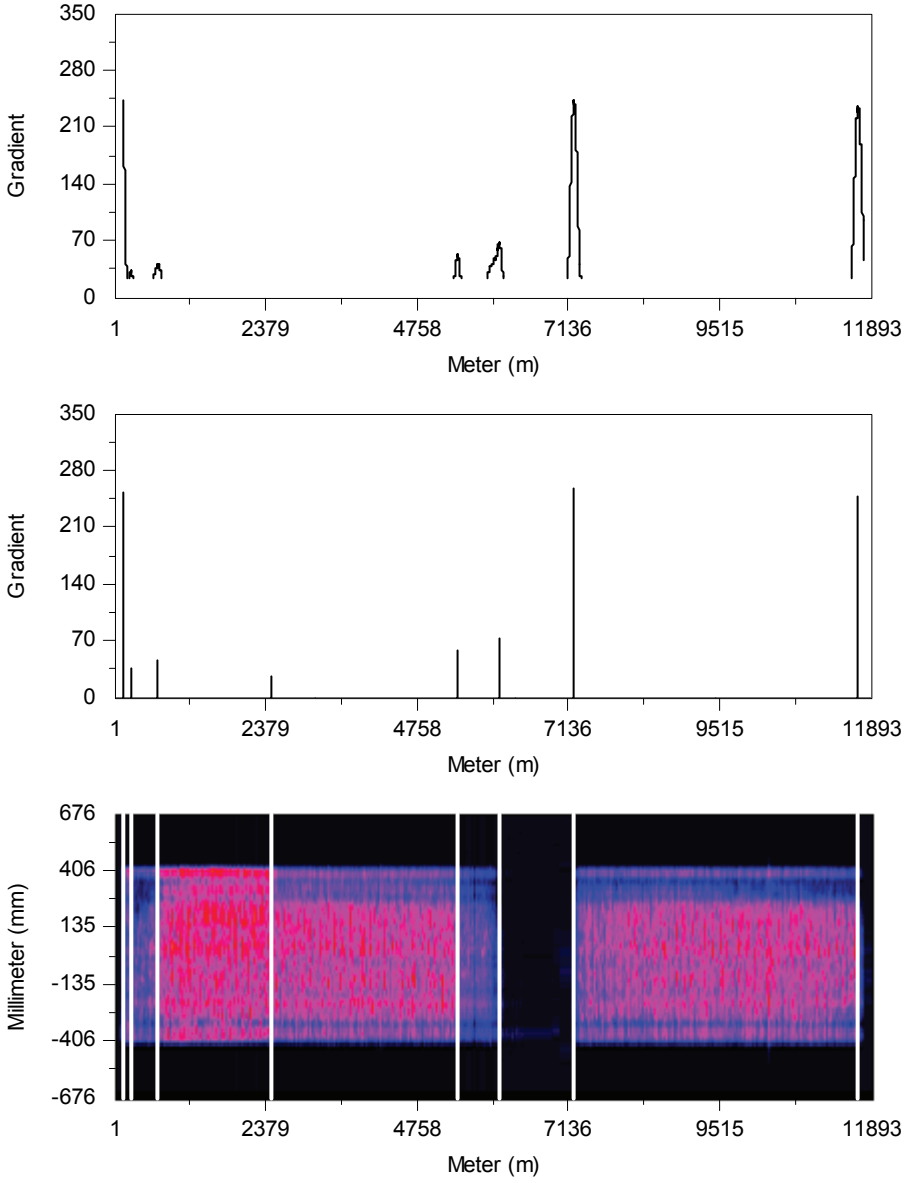

Fig. 7. Final steps of the detection process. (a) thresholding of the projection, (b) resulting position of the edges as the maximums of every peak, (c) segmented image

the difference operator. This process is carried out in real time with the infrared profile acquisition, detecting changes in the temperature pattern shortly after they appear.
The implementation of the segmentation method was successfully tested to fit the real time requirements imposed by a line acquisition rate of 100 Hz (10 ms period).

The configuration parameters of the algorithm are the following:

- Operator length (N).
- Projection power (P).
- Threshold level (T).

The results of the segmentation depend on the use of the proper values for these configuration parameters.

4. Tuning of the pattern detector

In order to tune the pattern detection process the best configuration for the parameters N, P, and T must be found.

The approach proposed to carry out automatic tuning of the pattern detection process is by means of evolutionary computation. This kind of computation method encompasses a variety of population-based problem solving techniques that mimic the biological process of Darwinian evolution, based on the principle of natural selection. Evolutionary algorithms provide versatile problem-solving mechanisms for search, adaptation, learning, and optimization in a variety of application domains (Bhandarkar & Zhang, 1999). The automatic segmentation tuning proposed in this work uses a genetic algorithm (Holland, 1992; Goldberg, 1989), an important member of the wider class of evolutionary algorithms which has been successfully used in the image processing field (Chun & Yang, 1996; Bhanu at al., 1995; Andrey, 1999; Pignalberi et al., 2003).

A genetic algorithm (GA) is an adaptive procedure that searches for viable solutions using a collection of search points, known as population, in order to maximize desirable criterion (Chun & Yang, 1996). Each search point, or member of the population, is known as an individual, and is represented as a chromosome encoded as a string of genes which are used to codify parameters. During iterations, each individual is evaluated and combined with others on the basis of its overall quality.

In this case, each chromosome contains the information about a configuration for the parameters of the segmentation algorithm. The quality of the chromosome is defined as the result provided by the combined objective function.

The first issue which must be defined in order to apply the genetic algorithm is the way the chromosomes are codified. Chromosomes contain information about parameters of the problem whose optimal values must be found. In this case, these values are the parameters of the segmentation process: N, P, and T. Each parameter is codified as a floating point number, thus, the chromosome is a vector of three numbers, as is represented in (8) for a generic chromosome i.

$$C_i = \left[N_i, P_i, T_i \right] \tag{8}$$

It is interesting to note that chromosomes are usually codified using binary methods; however, the use of floating point numbers has proved to provide similar or even better results than the binary codification for classical problems (Haupt & Haupt, 2003).

In this case, the population is defined as an array of 100 individuals, each represented by a chromosome which is initially filled with random numbers. Individuals are the search points of the genetic algorithm, and their quality is evaluated through Eq. (9), where C is a chromosome, which codifies the information about N, P and T, and OF is the objective function which indicates the success level of the segmentation using that parameter set.

$$Quality(C) = OF(N_i, P_i, T_i) \tag{9}$$

The genetic algorithm used is an iterative process which repeats the following four steps: natural selection, pairing, crossing, and mutation. These steps are described below.

4.1 Natural selection

The natural selection process decides which chromosomes in the population are fit enough to survive and possibly produce offspring in the next generation. To carry out this task, the quality of every chromosome in the population is calculated. Then, the array of chromosomes is sorted. Only the best half of the chromosomes survives (elitism), the rest are discarded to make room for the new offspring.

4.2 Pairing

The surviving chromosomes form the mating pool. The pairing process randomly creates pairs of fathers and mothers from this pool. Each pair produces two offspring which inherit traits from each parent. Enough pairs are created to fill the room left by the discarded chromosomes. In addition, the parents survive to form part of the next generation.

4.3 Crossing

Crossing is the process which produces offspring as a combination of the parents. Many different approaches for crossing have been tested (Michalewicz, 1994). In this case, a combination of blending (Radcliff, 1991) and extrapolation (Wright, 1991) is applied. The pseudocode of the crossing method can be seen in Algorithm 1.

```
function crossover(chromosome f, chromosome m)
  : chromosome o1, o2
begin
  beta = random[0, 1];

  switch (random_int[0, 1, 2])
  begin
    case 0: // N
      No1 = Nf - beta*(Nf - Nm);
      Po1 = Pf * random[0.5, 1.5];
      To1 = Tf * random[0.5, 1.5];

      No2 = Nm + beta*(Nf - Nm);
      Po2 = Pm * random[0.5, 1.5];
      To2 = Tm * random[0.5, 1.5];
    case 1: // P
      // Similar for P
      ...

    case 2: // T
      // Similar for T
      ...

  end_switch
end_function
```

Algorithm 1. Crossover strategy

4.4 Mutation

A common problem in any optimization technique setting out to find the global optimum is how to deal with local maximums. To avoid this problem, genetic algorithms force the exploration of other areas of the solution space by randomly introducing changes or mutations, in some of the chromosomes. The mutation method applied in this case mutates 5% of the population per iteration. The mutated chromosomes are selected randomly from the new generation resulting from the crossing process. The mutation process of a chromosome consists of the modification of one of its genes.

4.5 Objective function

Different evaluation methods for image segmentation which could be used as an objective function for the segmentation method have been proposed. (Zhang, 1996) proposes a classification of existing methods as "analytical", "empirical goodness", and "empirical discrepancy". The empirical discrepancy methods provide a value which indicates the similarity between the segmentation results and the ground truth. It is esteemed to be the most suitable method to be used as the objective function.

Jaccard (Sneath & Sokal, 1973) proposed a metric (JC) for classification purposes which has also been used as an empirical discrepancy method (Rosin & Ioannidis, 2003). This metric is defined in Eq. (10), where N_{TP} is the number of true positive detections, that is, the number of pixels correctly defined as edge pixels, N_{FP} is the number of false positive detections, that is, the number of pixels erroneously defined as edge pixels, and N_{FN} is the number of false negative detections, that is, the number of pixels erroneously defined as non-edge pixels.

$$JC = \frac{N_{TP}}{N_{TP} + N_{FP} + N_{FN}} \tag{10}$$

JC is a suitable method to be used as the objective function; therefore it will be used in this work.

The ground truth, necessary to determine the effectiveness of a detection method, is created by manually segmenting the images in a test set. This ground truth will be used to calculate the objective function (JC) during the tuning of the parameters of the pattern detector.

4.6 Results

After 250 iterations the best chromosome codifies the following parameter set:

- N: 118.
- P: 13.810.
- T: 5.869e12.

Fig. 8 and Fig. 9 show the infrared profile patterns detected in two images using the configuration obtained in the tuning procedure.

5. Feature extraction

Features extracted from an object aim to characterize the object to be recognized by measurements whose values are very similar for objects in the same category, and very different from objects in different categories (Duda et al., 2001). This leads to the idea of seeking distinguishing features.

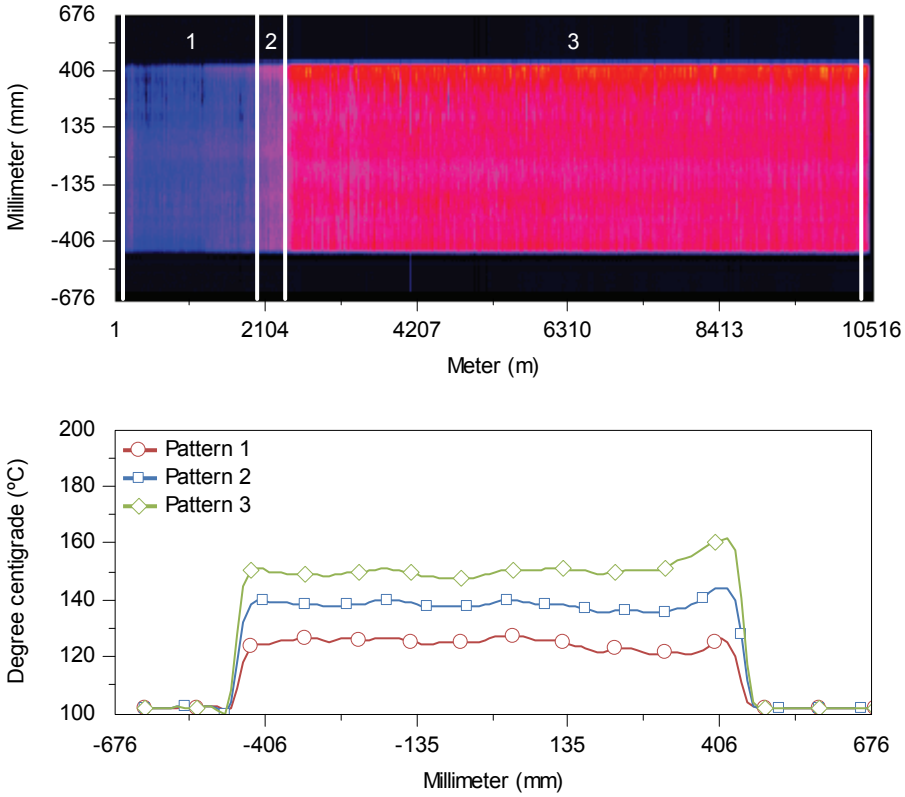

Fig. 8. Infrared profile patterns detected in image 1. (a) Segmented image, (b) infrared profile patterns for each segmented region

The proposed approach in this work is to extract features is by means of a polynomial fit. In particular, the shape of the infrared profile will be approximated by orthogonal polynomials (Abramowitz & Stegun, 1972). This approach has several advantages, including the elimination of the low frequency components of the signal (noise), and a reduction of the amount o information about the profile (Mukundan, 2004). However, the most important advantage of this approach is that the coefficients of the polynomials can be used to effectively describe the shape of the profile pattern.

To carry out the polynomial fit, several alternatives are available, including Chebyshev or Hermite orthogonal polynomials. However, in this case, Gram polynomials (sometimes called discrete Legendre orthogonal polynomials), are used due to their simplicity and accuracy.

Gram polynomials can be calculated using Eq. (11).

$$P_m(i) = c_{mN} \sum_{j=0}^{m} \frac{(-1)^j (m+j)^{2j}}{(j!)^2} \frac{i^j}{(N-1)^j} \tag{11}$$

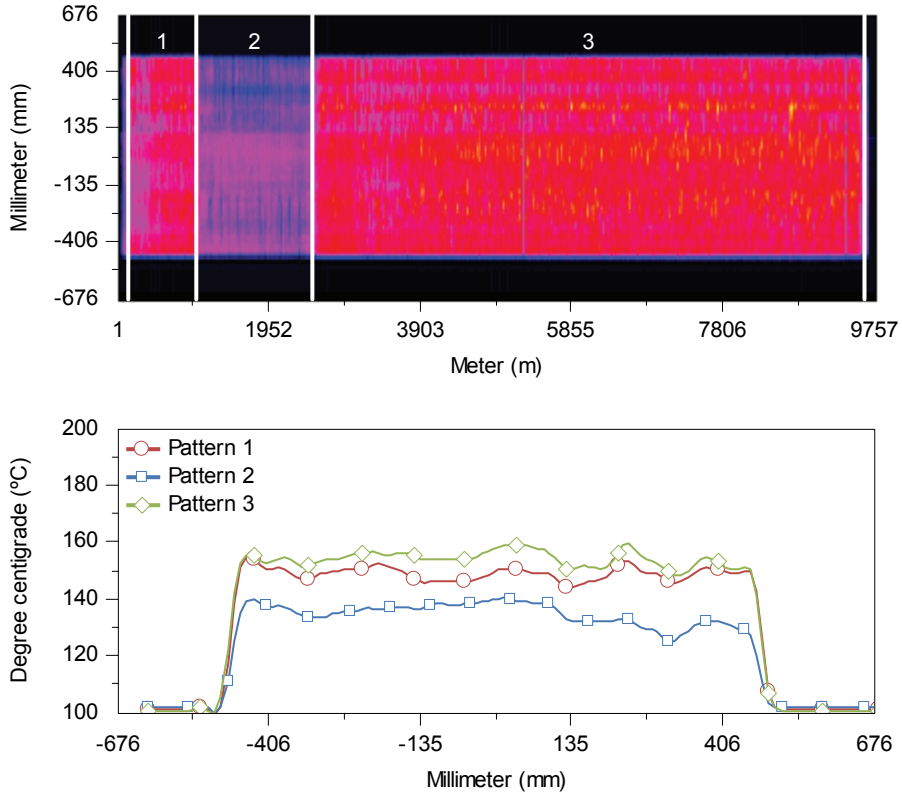

Fig. 9. Infrared profile patterns detected in image 2. (a) Segmented image, (b) infrared profile patterns for each segmented region

Gram polynomials, with c_{mN}=1, are constructed, for N equally spaced points in the interval [-1, 1] by the recurrence relationship shown in Eq. (12).

The matrix, X, consisting of the first p orthogonal polynomials evaluated at N points can be seen in (13). The profile or shape, Ω, can be expressed as (14), where ε consists of terms of order p+1 and higher (as a polynomial of order N-1 will match the measurements at the N data points), and c is the vector of coefficients of the orthogonal polynomials.

$$
\begin{aligned}
&P_{-1}(i) = 0 \\
&P_0(i) = 1 \\
&P_j(i) = \alpha(i,j)P_{j-1}(i) - \beta(j)P_{j-2}(i) \qquad j \geq 1 \\
&\alpha(i,j) = \frac{(N-1)(2j-1)}{j(N-j)}\left(1 - \frac{2i}{N-1}\right) \qquad i = 1,\ldots,N \\
&\beta(j) = \frac{(j-1)(N-1+j)}{j(N-j)}.
\end{aligned}
\tag{12}
$$

The least-squares estimate of the parameter vector c can be seen in (15).

$$\hat{\mathbf{c}} = \left(\mathbf{X}\mathbf{X}^{\mathrm{T}}\right)^{-1}\mathbf{X}\boldsymbol{\Omega} \equiv \mathbf{Q}\boldsymbol{\Omega} \tag{15}$$

Thus, the Gram polynomial approximation of the profile shape can be given by (16), where X^T is a diagonal matrix.

$$\hat{\boldsymbol{\Omega}} = \mathbf{X}^{\mathrm{T}}\mathbf{Q}\boldsymbol{\Omega} \tag{16}$$

The main advantage of the representation using orthogonal polynomials is that the polynomial coefficients, Cj, can be calculated independently of each other. If more coefficients are needed, the next (p+1) coefficient can be determined from Eq. (17), hence more coefficients can be added without affecting those already calculated.

$$\hat{c}(p+1) = \frac{1}{\mathbf{P}_{p+1}^{\mathrm{T}}\mathbf{P}_{p+1}}\mathbf{P}_{p+1}^{\mathrm{T}}\boldsymbol{\Omega} \tag{17}$$

From the Gram Polynomial, coefficients Ci can be used as features to describe effectively the shape of the profile. C0 is the constant coefficient and describes the average of the profile. C1 is the coefficient of the first order polynomial and describes the leveling of the profile, and thus, the symmetry when it is null. C1 will be positive when the temperature on the left border is higher than the one on the right border and negative otherwise. C2 is the coefficient of the second order polynomial and describes the curvature of the profile, which will be positive when the temperature of the borders is higher than the temperature in the middle or negative otherwise. Depending on the applications, more coefficients could be used, but these three coefficients are enough to describe common features of infrared profiles patterns.

Before extracting features from infrared profiles patterns, background and foreground need to be separated to avoid an incorrect fit. This process can be carried out using any thresholding technique (Sezgin & Sankur, 2004). In this work, the limits of the foreground were calculated using the zero crossing positions of the second derivative of the profile.

Fig. 10 shows the representation of the Gram polynomial fit for the infrared profile patterns detected in Fig 8 and Fig. 9. Table 2 shows the features extracted from these patterns.

Features shown in Table 2 contain very interesting information. For example, the right border in pattern 3 of image 1 has higher temperature than the left border. Pattern 2 of image 2 has the left border with higher temperature than the right border, and also, the temperature in the middle is higher than in the borders. Many other conclusions could be easily drawn form the extracted features.

These features make it possible to develop a pattern classifier. They can also be used directly by the manufacturing control systems to correct anomalous situations in real-time.

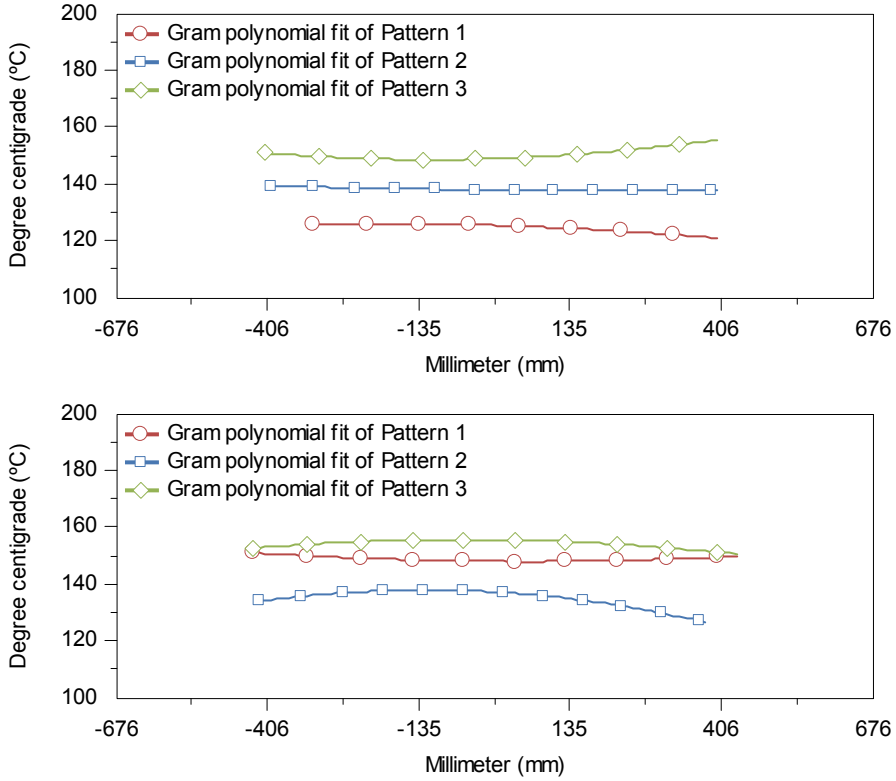

Fig. 10. Gram polynomial fit. (a) patterns in image 1, (b) patterns in image 2

Image	Pattern	Average (C0)	Leveling (C1)	Curvature (C2)
1	1	124.851	2.438	-1.150
1	2	138.424	0.632	0.481
1	3	150.616	-2.355	2.818
2	1	149.077	0.621	1.566
2	2	135.296	3.633	-4.637
2	3	154.526	1.023	-2.636

Table 2. Features extracted from the detected patterns

6. Conclusions

In this work, a method to detect infrared profiles patterns in real-time is proposed. The method is based on real-time segmentation of infrared images acquired using an infrared line-scanner. The segmentation is based on the detection of edges which indicate the change of the current infrared profile pattern. The segmentation consists of the calculation of the gradient, its projection, and its thresholding. These three steps are designed to be applied in real-time. Therefore, the information about the current infrared profile pattern can be used

during manufacturing. A procedure to tune the pattern detector based on evolutionary computation is also proposed. The procedure produced the best configuration parameters of the proposed detector. The results of the pattern detector meet the functional and the real-time requirements.

Methods to extract distinguishing features from infrared patterns are also explored in this work. The results obtained indicate that polynomial fit using Gram orthogonal polynomials provide a compact and meaningful description of infrared profile patterns. The coefficients of the polynomials can describe interesting features, such as average, levelling, or curvature. These features could be easily used in many types of applications which aim to classify the patterns in different groups. These features are also an excellent method to describe images with only a few numbers, which can make the analysis or the storage of the information much more effective.

The proposed methods are very likely to find potential applications in a number of different areas, such as robotics, manufacturing control, or any other applications based on the processing of a stream of infrared profiles in real-time. Furthermore, even if the proposed method has been described for infrared images, its use with images taken from the visible spectrum is straightforward.

7. References

Abramowitz, M. & Stegun, I. A. (1972). Handbook of Mathematical Functions with Formulas, Graphs, and Mathematical Tables, Dover Publications, ISBN: 0486612724.

Andrey, P. (1999). Selectionist relaxation: genetic algorithms applied to image segmentation. Image and Vision Computing, Vol. 17, No. 3-4, 175-187.

Canny, J. (1986). A computational approach to edge detection. IEEE Transactions on Pattern Analysis and Machine Intelligence, Vol. 8, No. 6, 679-698.

Bhanu, B.; Lee, S. & Ming J. (1995). Adaptive image segmentation using a genetic algorithm. IEEE Transactions on Systems, Man and Cybernetics, Vol. 25, No. 2, 1543-1567.

Bhandarkar, S. M. & Zhang, H. (1999). Image Segmentation Using Evolutionary Computation. IEEE Transactions on Evolutionary Computation, Vol. 3, No. 1, 1-21.

Chun, D. N. & Yang H. S. (1996). Robust Image Segmentation Using Genetic Algorithm with a Fuzzy Measure. Pattern Recognition, Vol. 29, No. 7, 1195-1211.

Duda, R. O.; Hart, P. E. & Stork, D. G. (2001). Pattern Classification, Wiley-Interscience, ISBN: 0471056693, New York.

Goldberg, D. E. (1989). Genetic Algorithms in Search, Optimization, and Machine Learning, Addison-Wesley, ISBN 0201157675, Reading, MA.

Gonzalez, J. A.; Obeso, F.; García, D. F.; Usamentiaga, R. & Falessi, R. (2002). Application of thermographic analysis for the detection of longitudinal defects in cold mills. Revue de Metallurgie. Cahiers D'Informations Techniques, Vol. 99, No. 6, 537-543.

Haupt, R. L. & Haupt, S. E. (2004). Practical genetic algorithms, Wiley-Interscience, ISBN: 0471188735, New York.

Holland, J. H. (1992). Adaptation in Natural and Artificial Systems, MIT Press, ISBN 0-262-58111-6, Cambridge, MA

Michalewicz, Z. (1994). Genetic Algorithms + Data Structures = Evolution Programs, Springer-Verlag, ISBN: 3540606769, Berlin.

Mukundan, R. (2004). Some Computational Aspects of Discrete Moments. IEEE Transactions on Image Processing, Vol. 13, No. 8, 1055-1059.

Pignalberi, G.; Cucchiara, R.; Cinque, L. & Levialdi S. (2003). Tuning range image segmentation by genetic algorithm. Eurasip Journal on Applied Signal Processing, Vol. 2003, No. 8, 780-790.

Pratt, W. K. (2001). Digital Image Processing, Wiley-Interscience, ISBN: 0471374075, New York.

Radcliff, N. J. (1991). Forma analysis and random respectful recombination, Proc. 4th Int. Conf. on Genetic Algorithms, pp. 222-229, San Marco CA, 1991, Morgan Kauffman.

Rosin, P. L. & Ioannidis E. (2003). Evaluation of global image thresholding for change detection. Pattern Recognition Letters, Vol. 24, No. 14, 2345-2356.

Sezgin, M. & Sankur, B. (2004). Survey over image thresholding techniques and quantitative performance evaluation. Journal of Electronic Imaging, Vol. 13, No. 1, 146-168.

Sneath, P. & Sokal R. (1973). Numerical Taxonomy, The principle and practice of numerical classification, W H Freeman & Co, ISBN: 0716706970, San Francisco.

Wright, A. H. (1991). Genetic algorithms for real parameter optimization. Foundations of Genetic Algorithms, Vol. 1, 205-218.

Zhang, Y. J. (1996). A Survey on Evaluation Methods for Image Segmentation. Pattern Recognition Elsevier Science, Vol. 29, No. 8, 1335-1346.